Hindawi Publishing Corporation
Mathematical Problems in Engineering
Volume 2015, Article ID 538176, 12 pages
http://dx.doi.org/10.1155/2015/538176

*Research Article*

# Prediction Method of the Fuel Consumption of Wheel Loaders in the V-Type Loading Cycle

**Wenxing Ma,[1] Yubo Zhang,[1] Chunbao Liu,[1] and Songlin Wang[2]**

[1]*School of Mechanical Science and Engineering, Jilin University, Changchun 130022, China*
[2]*Guangxi Liugong Machinery Co. Ltd., Liuzhou, Guangxi 545007, China*

Correspondence should be addressed to Chunbao Liu; liuanbc@126.com

Received 23 June 2015; Accepted 27 September 2015

Academic Editor: Reza Jazar



Wheel loaders in the V-type loading cycle are characterized by complicated loading conditions, nonlinear power-train system, and time-variable engine power distribution. Therefore, it is difficult to predict the fuel consumption of wheel loaders in the V-type loading cycle. The static matching methods cannot provide fuel consumption prediction for the loading cycle. In this paper, the prediction method and model of the fuel consumption for wheel loaders in the V-type loading cycle were proposed. Firstly, the hydraulic system data were tested when a wheel loader loaded three different materials in a typical V-type loading cycle. Secondly, the tested data were filtered by the 8th-order Butterworth filter and the dimensionless power deduction equations of hydraulic power system for loading three different materials were obtained by Gaussian and linear fitting based on the filtered data in the loading cycle. Finally, fuel consumption was obtained with the compiling dynamic calculation program as well as input parameters of tested vehicle speed, throttle parameter, and the dimensionless equation. The simulation results agreed well with experiment results. Dynamic calculation program is applicable to calculate loading economy and can provide academic guidance for wheel loader's design and optimization.

## 1. Introduction

V-type loading cycle fuel consumption is the most significant economic index for wheel loaders. The typical V-type loading cycle, as shown in Figure 1, consists of V1 phase (moving forward to material), V2 phase (loading material), V3 phase (returning to the initial position from material), V4 phase (driving full-load loader to transporter), V5 phase (unloading material), and V6 phase (returning to the initial position from transporter) [1].

In the power-train system of a wheel loader (Figure 2), the engine power is transported to three different parts: accessories, the hydraulic system, and the driveline system. In the V-type loading cycle, driving resistance and digging resistance are mainly loaded on the wheel loader. One loading cycle may contain one single load or multiple loads. The engine power distribution is closely related to the external workloads. Wheel loaders in the V-type loading cycle are characterized by complicated loads, nonlinear power-train system, and time-variable engine power distribution. Therefore, it is difficult to predict the fuel consumption [2].

Wheel loaders in the V-type loading cycle had been extensively studied. Filla et al. developed the dynamic simulation platform for wheel loader vehicle performance, economy, and operability by combining the automatic control model with the operator model [1, 3, 4]. Hemami planned an optimal digging path to minimize the digging force and enhance the loading economy and efficiency [5]. Yossawee et al. proposed the method to calculate initial and final positions with the symmetric Clothoid curve and planned a V-type loading cycle path reasonably [6]. Wu et al. got an optimal loading path by means of test and theory analysis and then controlled the bucket along the path to improve fuel efficiency and operability [7–9].

The V-type loading cycle was mainly obtained by test and fuel consumption prediction was seldom obtained through simulation. Bohman obtained a simple model by dividing the cycle into different parts to calculate V-type loading cycle fuel

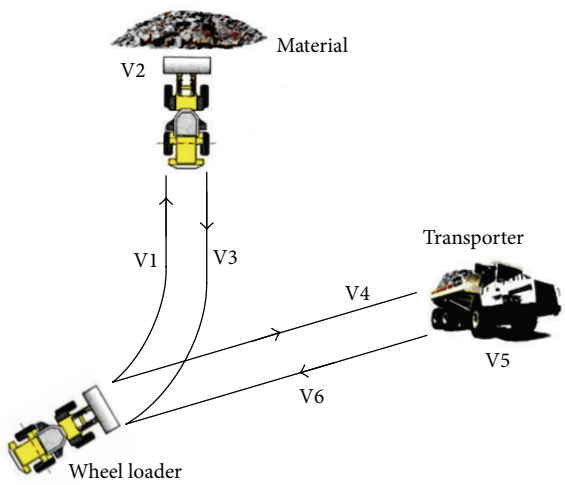


Figure 1: V-type loading cycle.

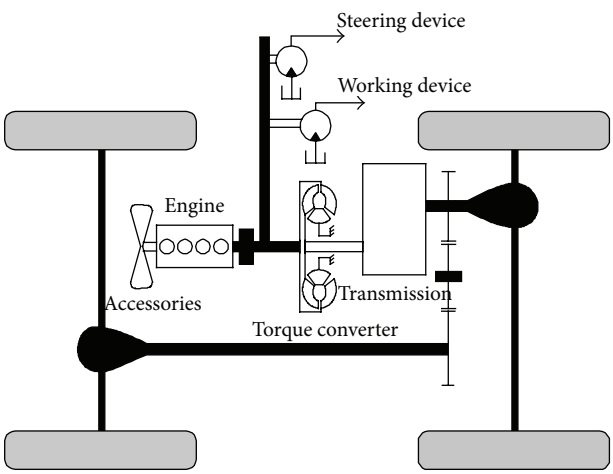


Figure 2: Power-train system of wheel loader.

consumption, but the relative error was large and generally ranged from 10% to 20% [10]. This paper aims to develop a method to predict the V-type loading fuel consumption accurately.

Engine power distribution in the V-type loading cycle is the key to study fuel consumption of wheel loader. The power from engine is mainly to balance digging resistance and driving resistance and the digging resistance balanced by the hydraulic system is complicated and unpredictable. Takahashi got a curve of force when the loader was digging some materials by tests and the simulation method and the curve showed the complex nonlinear change [11]. However, the power transportation loss in the hydraulic system was unknown. Therefore, it was impossible to calculate the hydraulic system power. Filla got the power distribution map by simulation [12]. Debeleac got the engine power distribution of the wheel loader working in the V-type loading cycle by means of the theoretical calculation with testing data of the hydraulic system [13]. In the paper, the hydraulic system power distribution characteristic was gotten by the mathematic calculation method [13].

The engine power of a wheel loader is generally diverted to the transmission system, the hydraulic system, and accessories. In this paper, engine power deduction is defined as the power obtained after subtracting the power diverted to the transmission system and can represent engine power distribution. Engine power deduction is widely used in static matching. In general, the static matching method can be expressed as

$$f\left(\alpha, R_d, F_f\right) = v. \tag{1}$$

It means that, at a certain gear, the vehicle velocity $v$ can be determined by three different parameters: throttle $\alpha$, power deduction $R_d$, and running resistance $F_f$. In other words, velocity reflects the running resistance of vehicle. The traditional static matching cannot be used to predict fuel consumption of a wheel loader in loading cycle. Equation (1) may be rewritten as

$$f\left(\alpha\left(t\right), R_d\left(t\right), v\left(t\right)\right) = Q_t\left(t\right). \tag{2}$$

Taking time-variable throttle $\alpha(t)$, engine power deduction $R_d(t)$, and velocity $v(t)$ as input parameters to compile dynamic calculation program based on the traditional matching program, we obtained fuel consumption ratio $Q_t(t)$ curve through the iterative matching. V-type loading cycle fuel consumption can be acquired by the accumulation method.

## 2. Dynamic Power Deduction in the V-Type Loading Cycle

*2.1. Test.* When the wheel loader works in the V-type loading cycle, the hydraulic system power varies with time. The pressure and flow of working pump and steering pump (red circle shown in Figure 3) on the output side of the gearbox are tested while the loader is digging sand, stone, and freestone. The sensor placement is shown in Figure 3. The pressure and flow signals were tested with pressure flow sensors. The inlets of working pump and steering pump were connected to the tank. Therefore, only one of the inlet pressure and flow should be tested. The testing controller could be used to collect the data. The collected data were stored in the internal storage unit of controller and the sampling frequency was set to be 100 HZ.

*2.2. Data Processing of Hydraulic System.* The signal of a wheel loader is a typical low-frequency signal and only stable flat pass band performance could ensure the integrity of the useful signal at the most. Therefore, IIR digital filter was chosen to process the data. Butterworth filter attenuation rate was slower than other IIR digital filters, but its attenuation rate was very flat without amplitude variation. The higher order means that its performance is closer to the ideal low-pass filter [14]. Squared magnitude response of Butterworth low-pass filter can be expressed by the following [15]:

$$\left|H\left(j\omega\right)\right|^2 = \frac{1}{1 + \left(\omega/\omega_c\right)^{2n}}, \tag{3}$$

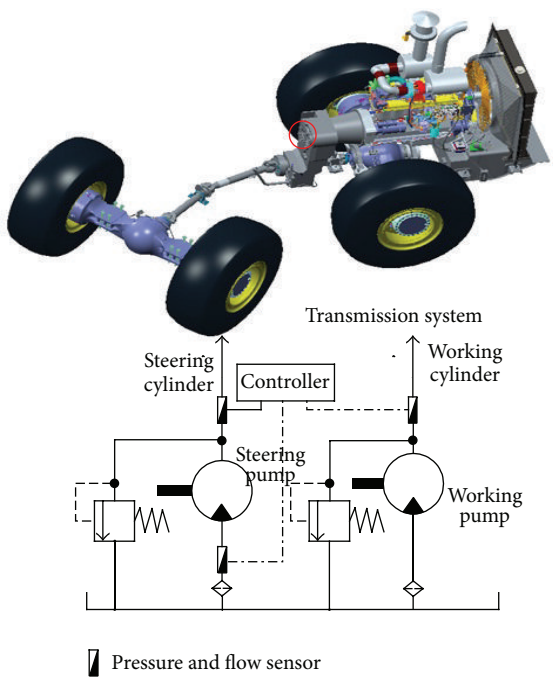


Figure 3: Testing principle.

Table 1: Analysis and comparison of the pressure data obtained before and after filtering.

| | Before filtering | | | After filtering | | |
|---|---|---|---|---|---|---|
| | $P_1$ | $P_2$ | $P_T$ | $P_1$ | $P_2$ | $P_T$ |
| AVG | 4.54 | 6.702 | 0.2027 | 4.539 | 6.709 | 0.2027 |
| SD | 5.484 | 5.042 | 0.071 | 5.421 | 4.874 | 0.07 |
| RMS | 7.119 | 8.387 | 0.2146 | 7.069 | 8.292 | 0.2145 |

where $n$ is the order of the filter and $\omega_c$ is the cutoff frequency of the low-pass filter.

The 8th-order butterwort low-pass filter with a cutoff frequency of 2 HZ was selected in order to filter the inlet and outlet pressure data of hydraulic pump when the wheel loader was used to load freestone material in the V-type loading cycle. The result is shown in Figure 3.

As shown in Figure 4, $P_1$ represents the outlet pressure of working pump; $P_2$ represents the outlet pressure of steering pump; $P_T$ represents the pressure of intake pipe. The mathematical statistics analysis indicated that the pressure signals of pump became smoother after filtering and that the completeness and accuracy of the filtered data were maintained (Table 1). The filtered data are more conducive to the model loading.

After processing the flow data of hydraulic pump in the same way, the curves are obtained and shown in Figure 5.

In Figure 5, $Q_1$ is the flow of working pump; $Q_2$ is the flow of steering pump.

*2.3. Power Deduction Calculation.* The power of hydraulic systems was calculated by pressure difference between the inlet and outlet flows of hydraulic pumps. The hydraulic system power shows the complicated change in V-type cycle and can be calculated as

$$P = \frac{\Delta p \cdot Q}{60 \cdot \eta}, \tag{4}$$

where $\Delta p$ is the differential pressure between the inlet and outlet pressures, $Q$ is the volume flow rate, and $\eta$ is the overall efficiency.

The ratio of hydraulic pump power to rated engine power plus the accessory power ratio equals the engine power deduction in the V-type loading cycle. Accessory power consumption is nonlinear. But limited by the condition of technical test, we have simplified the auxiliary power ratio whose number is 10% according to engineering experience. The engine power deduction can be calculated by (5). The engine power deduction curve is shown in Figure 6. Consider

$$R_d = \frac{P_g + P_z}{P_{ee}} \times 100\% + R_a, \tag{5}$$

where $R_d$ is the engine power deduction, $R_a$ is the accessory deduction ratio which is 10% in this paper, $P_g$ is working pump power, $P_z$ is steering pump power, and $P_{ee}$ is the rated engine power.

In Figure 6, the power deduction in the whole V-type loading cycle is complicated and the data have no linear relationship with time in each phase. Therefore, fitting engine power deduction data in each phase with nonlinear regression function can provide good fitting effects.

In the test, we tested the loader's related data when loading three different materials (freestone, sand, and stone) in the V-type cycle. It can be considered that working conditions of a wheel loader remain unchanged when the same driver operates the same wheel loader except the V2 phase. That is to say, the engine power deduction remains unchanged except in the V2 phase. And when loading different materials, bucket movement and vehicle velocity show little differences except temporal variations.

Through fitting each phase in loading cycle with Matlab Cftool as well as a lot of mathematic tests, we found that Gaussian function could accurately fit the engine power deduction curve and that linear fitting could ensure the function continuity between two working phases. Gaussian function and linear function are, respectively, expressed as follows:

$$\begin{aligned} f(x) &= \sum_{i=1}^{n} a_i \cdot \exp\left(-\left(\frac{x - b_i}{c_i}\right)^2\right), \\ f(x) &= \sum_{i=1}^{n} d_i \cdot x^{n-i}. \end{aligned} \tag{6}$$

Table 2 shows the coefficients of dimensionless power deduction equation when loading freestone material. $a$, $b$, and $c$ are the Gaussian fitting factors and $d$ is the linear fitting factor.

In the power deduction curve based on test data (Figure 7), the fitting equation curve and the relative error

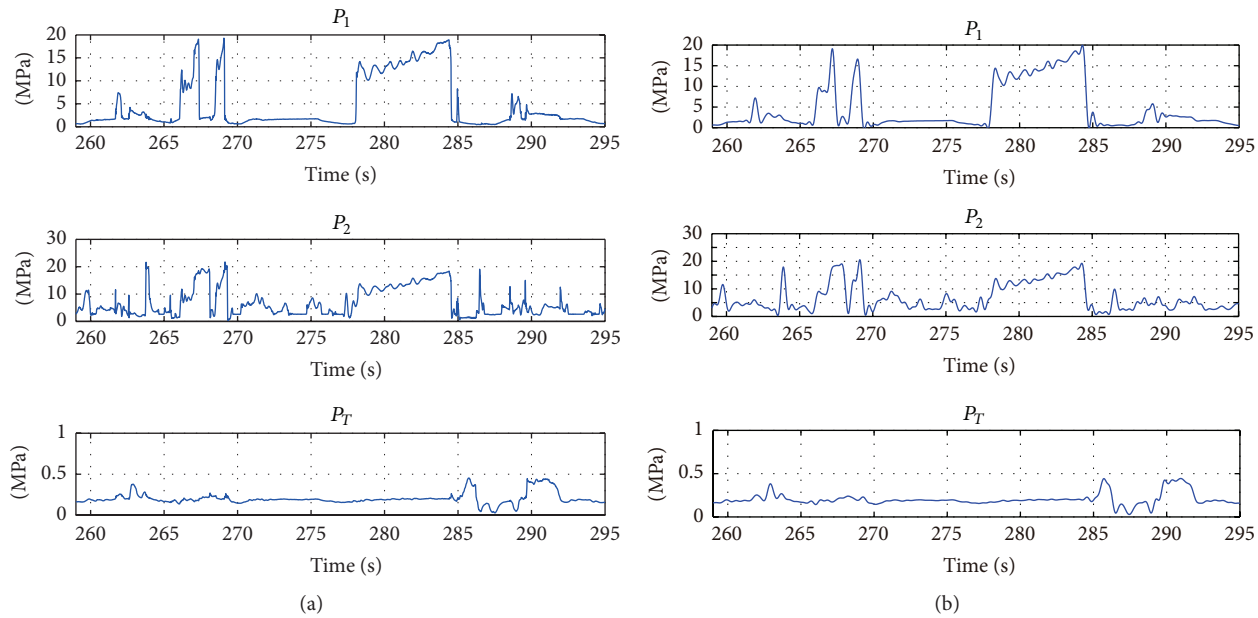


Figure 4: (a) Testing pressure data and (b) filtered pressure data.

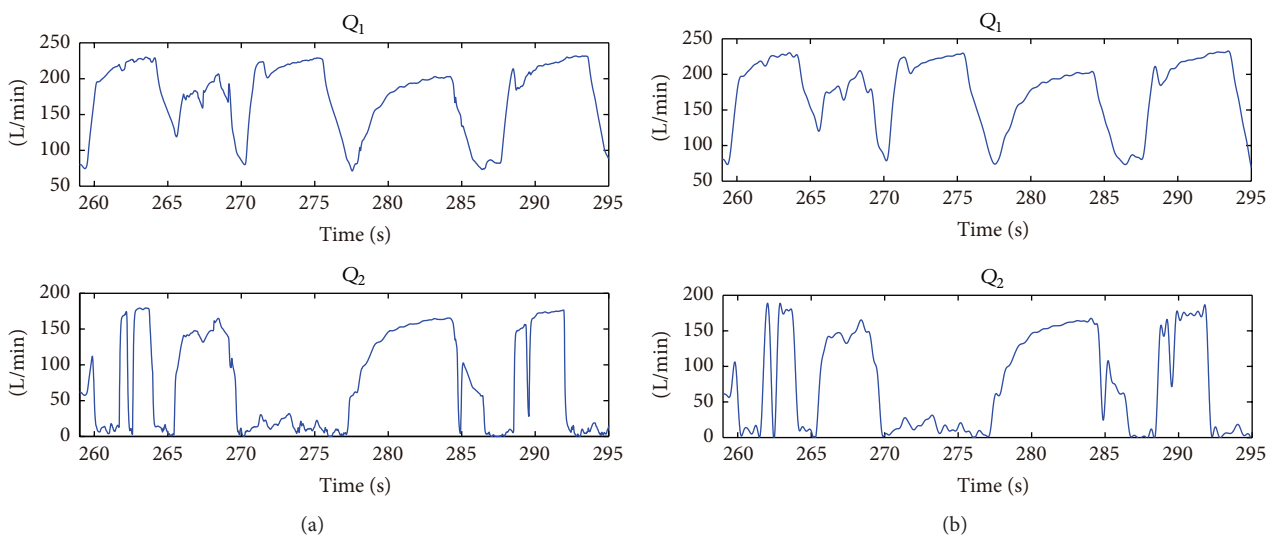


Figure 5: (a) Testing flow data and (b) filtered flow data.

directly show that the equation has accurately described the power deduction.

In the same way, we fit the engine power deduction data when loading sand material and stone material in V2 phase via Gaussian and linear fitting (Table 3 and Figures 8 and 9).

## 3. Fuel Consumption Calculation in the V-Type Loading Cycle

The calculation method of fuel consumption in the V-type loading cycle is described as follows.

*3.1. Mathematic Calculation Method.* In the V-type loading cycle, wheel loader's fuel consumption ratio $Q_t$ (mL/s) in different time can be obtained via static matching calculation. Each additional period $\Delta t = 0.1$ s is set as a small interval and the fuel consumption ratio $Q_t$ (mL/s) multiplied by the $\Delta t$ is equal to the fuel consumption within the interval, $Q_i$. This is the approximate calculation. The total fuel consumption $Q_1$ (mL) from $t_0$ to $t_1$ can be obtained as

$$Q_1 = \frac{1}{2}\left(Q_{t0} + Q_{t1}\right) \cdot \Delta t, \tag{7}$$

where $Q_{t0}$ is the fuel consumption at time $t_0$ when vehicle velocity is $v_{t0}$ and $Q_{t1}$ is the fuel consumption at time $t_1$ when vehicle velocity is $v_{t1}$.

Table 2: The coefficients of dimensionless power deduction equation for working conditions of loading freestone material.

| | Coefficients | 1 | 2 | 3 | 4 | 5 | 6 | 7 | 8 |
|---|---|---|---|---|---|---|---|---|---|
| V1 | $a$ | 24.03 | 21.31 | 13.28 | 9.796 | 9.466 | 6.36 | | |
| | $b$ | 4.811 | 2.959 | 3.408 | 0.793 | 3.837 | 4.279 | | |
| | $c$ | 0.179 | 0.223 | 15.597 | 0.176 | 0.234 | 0.235 | | |
| | $d$ | 2.698 | −33.03 | 112.8 | | | | | |
| V2 | $a$ | 49.02 | 48.33 | 33.14 | 29.92 | 12.52 | 27.17 | | |
| | $b$ | 2.223 | 4.003 | 3.628 | 2.904 | −13.758 | 1.432 | | |
| | $c$ | 0.344 | 0.257 | 0.194 | 0.271 | 52.882 | 0.404 | | |
| | $d$ | −5.332 | 65.5 | −187.2 | | | | | |
| V3 | $a$ | 2.539 | 1.587 | 2.237 | 0.6603 | 0.4072 | 0.953 | 3.311 | 13.69 |
| | $b$ | 0.342 | 2.229 | 4.141 | 3.421 | 1.824 | 4.557 | 6.475 | 1.844 |
| | $c$ | 0.312 | 0.213 | 0.317 | 0.567 | 0.182 | 0.208 | 0.245 | 8.411 |
| | $d$ | 12.67 | −156.6 | 491.9 | | | | | |
| V4 | $a$ | 14.69 | 45.61 | 8.583 | 19.56 | 55.68 | −4.651 | 14.5 | 4.818 |
| | $b$ | 6.307 | 6.013 | 4.67 | 1.125 | 3.688 | 3.213 | 0.3969 | 3.96 |
| | $c$ | 0.1631 | 0.9838 | 0.4431 | 1.148 | 2.572 | 0.008405 | 0.2713 | 0.2311 |
| | $d$ | 383.5 | −5204 | 17660 | | | | | |
| V5 | $a$ | 8.936 | 8.414 | 4.97 | 7.579 | 25.68 | 8.361 | | |
| | $b$ | 0.212 | 1.647 | 0.655 | 1.180 | −3.325 | 2.050 | | |
| | $c$ | 0.189 | 0.214 | 0.247 | 0.407 | 3.251 | 0.284 | | |
| | $d$ | −11.5 | 47.55 | −38.56 | | | | | |
| V6 | $a$ | −27.89 | 11.62 | 9.915 | 10.86 | 35.66 | 7.921 | 13.98 | 9.204 |
| | $b$ | 12.923 | 3.918 | 4.877 | 4.455 | 2.489 | 2.759 | 5.795 | −0.014 |
| | $c$ | 1.078 | 0.327 | 0.183 | 0.345 | 0.841 | 0.203 | 3.687 | 1.975 |

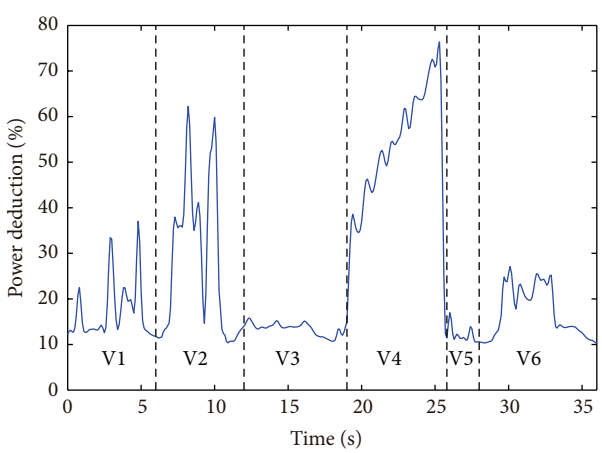


Figure 6: Power deduction curve when loading freestone material in the V-type loading cycle.

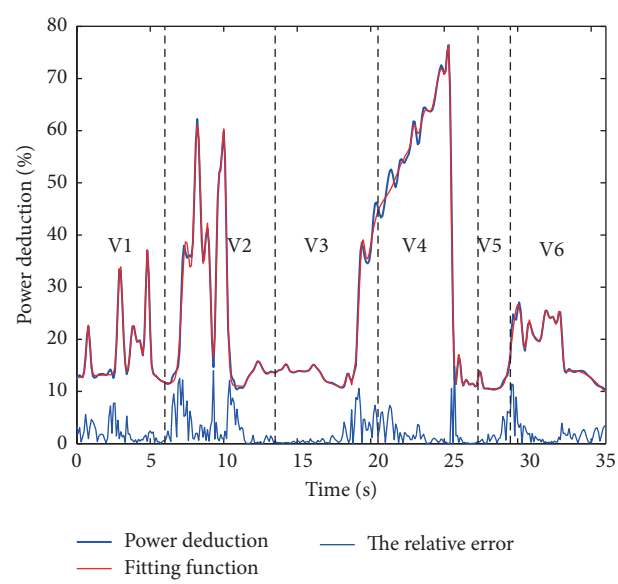


Figure 7: Comparison between the calculation curve and the fitting power deduction curve in the V-type loading cycle when loading freestone material.

As shown in Figure 10, the fuel consumption of each interval can be expressed as

$$Q_2 = \frac{1}{2}\left(Q_{t1} + Q_{t2}\right) \cdot \Delta t$$
$$\vdots \tag{8}$$
$$Q_n = \frac{1}{2}\left(Q_{t(n-1)} + Q_{tn}\right) \cdot \Delta t,$$

where $Q_{t2}, Q_{t3}, \ldots$, and $Q_{tn}$ are, respectively, fuel consumption at times $t_1, t_2, \ldots$, and $t_n$.

In the slowing down phase, a driver loosens engine throttle valve and brakes slightly and the torque converter

Table 3: The coefficients of power deduction equation in V2 phase when loading sand or stone material.

| Materials | Coefficients | 1 | 2 | 3 | 4 | 5 | 6 | 7 | 8 |
|---|---|---|---|---|---|---|---|---|---|
| Sand | $a$ | 50.08 | 24.27 | 10.48 | 41.7 | 4.175 | | | |
| | $b$ | 3.804 | 2.588 | 5.232 | 1.886 | 0.6637 | | | |
| | $c$ | 0.4567 | 0.4247 | 0.7816 | 1.642 | 0.2908 | | | |
| | $d$ | −8.361 | 100.9 | −290.8 | | | | | |
| Stone | $a$ | 44.45 | 41.83 | 30.88 | 24.53 | 25.76 | 68.51 | −16.24 | 18.93 |
| | $b$ | 2.367 | 4.635 | 5.481 | 3.773 | 1.544 | −13.196 | −0.017 | 3.033 |
| | $c$ | 0.300 | 0.637 | 0.313 | 0.301 | 0.385 | 14.608 | 0.294 | 0.311 |
| | $d$ | 2.006 | −25.65 | 93.34 | | | | | |

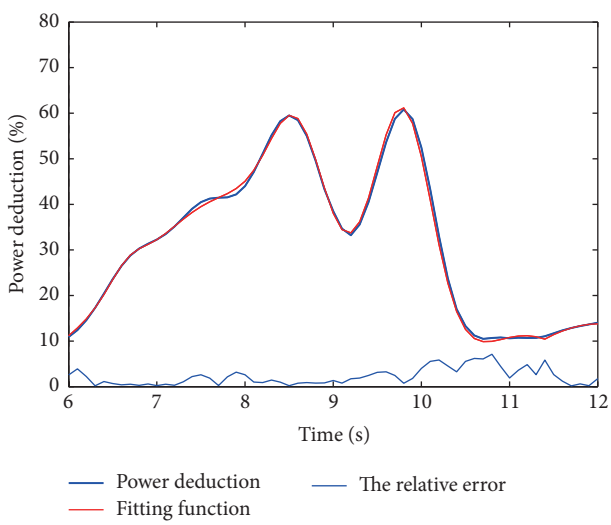


Figure 8: Power deduction curve in V2 phase when loading sand material.

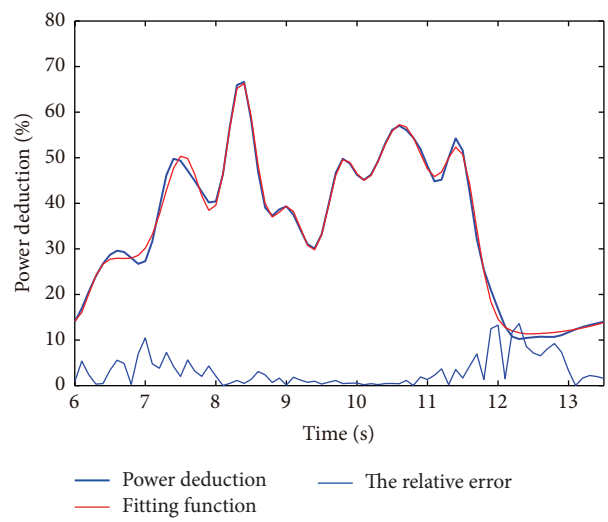


Figure 9: Power deduction curve in V2 phase when loading stone material.

may work in the reverse transfer condition that makes engine in idling state. Under this condition, the fuel consumption ratio is idling fuel consumption $Q_d$ (mL/s). The total fuel consumption $Q_f$ (mL) in reversed transmission condition equals the product of idling time $t_f$ (s) and $Q_d$:

$$Q_f = Q_d \cdot t_f. \tag{9}$$

Therefore, the total fuel consumption in the V-type loading cycle $Q$ can be calculated by

$$Q = \sum_{i=1}^{m} Q_i + Q_f, \tag{10}$$

where $m$ is the number of sections in which the torque converter works under the traction condition.

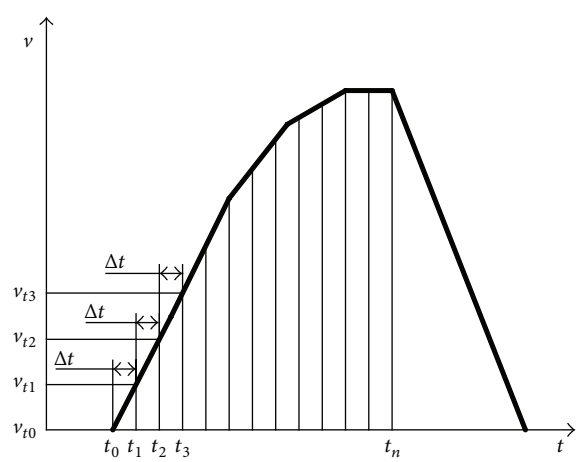


Figure 10: Calculation results of fuel consumption for traction working conditions.

*3.2. Dynamic Calculation.* Based on the abovementioned fuel consumption calculation method and the static matching program, we compiled a dynamic calculation program to acquire the vehicle traction characteristics and fuel consumption characteristics at different time and obtained the dynamic traction force and dynamic fuel consumption ratio in the whole V-type loading cycle phase. The block diagram of dynamic calculation is shown in Figure 11. The fuel consumption prediction model for wheel loaders in the V-type loading cycle is shown in Figure 12.

The simulation settings are as follows: fixed-step Bogacki-Shampine solver; step length of 0.1 s; the total iterative

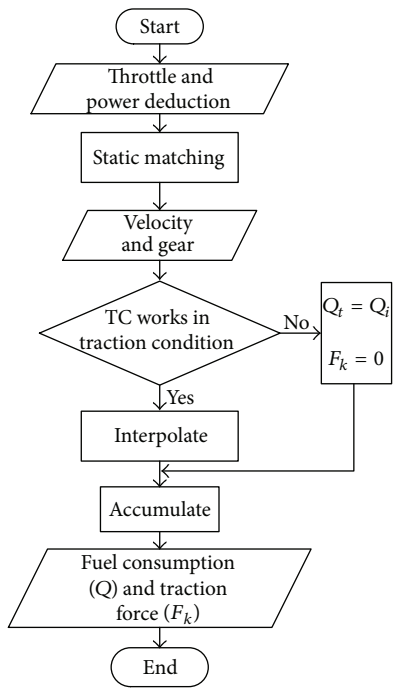


Figure 11: Block diagram of dynamic calculation.

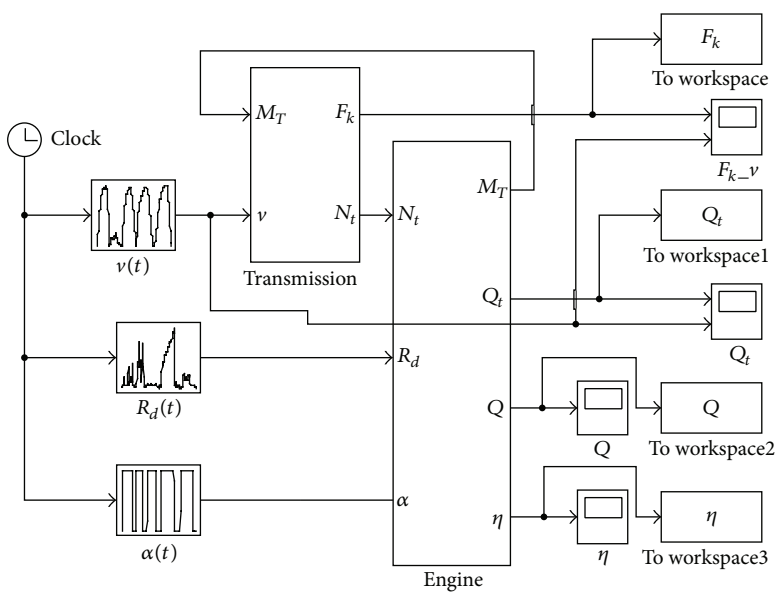


Figure 12: V-type loading cycle model for wheel loaders.

calculation time which is the time length of a V-type loading cycle. Taking the working conditions of loading freestone material as an example, the input parameters are shown in Figure 13. Velocity, throttle, and power deduction can be rebuilt based on the input parameters for different wheel loaders.

*3.3. Static Matching.* The static matching mentioned above is described as follows. If the engine power and throttle at the given time are known, the static matching performances between engine and torque converter, including common input characteristics, common output characteristics, traction characteristics, and fuel consumption characteristics at the time, can be acquired. The block diagram of static matching is shown in Figure 14. The vehicle traction characteristic shows the relationship between traction force and velocity at different gears. The fuel consumption characteristic shows the relationship between fuel consumption ratio and velocity at different gears.

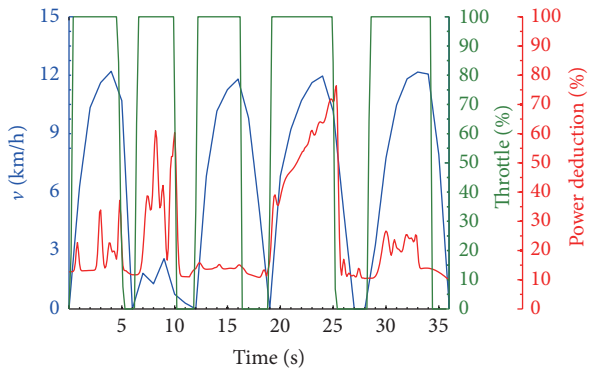


FIGURE 13: Input parameters.

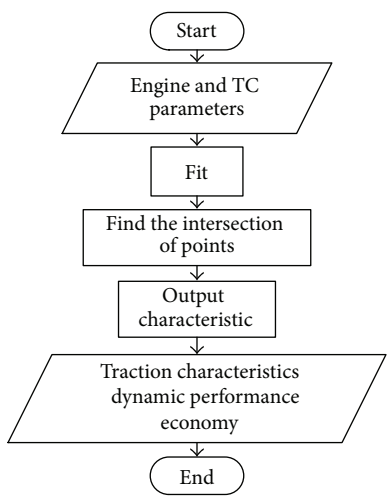


FIGURE 14: Block diagram of static matching.

After linear fitting with the testing data of engine and torque converter, the obtained fitting curves are, respectively, shown in Figures 15 and 16. Equations (11) and (12) express the engine throttle characteristics and original torque converter characteristics, respectively. Considering the environment conditions for engine experiment such as the temperature and humidity are similar with the conditions for V-type loading cycle, we neglect the influence of environmental factors on the performance of the engine. Consider

$$T_{e1} = \sum_{i=0}^{n} a_i \cdot n_e^{\,i} \quad (n_{e\_\min} \le n_e \le n_{e\_e}),$$
$$T_{e2} = b_1 \cdot n_e + b_0 \quad (n_{e\_e} < n_e \le n_{e\_\max}),$$
$$g_e = \sum_{i=0}^{n} c_i \cdot n_e^{\,i}, \tag{11}$$
$$P_e = T_e \cdot \frac{n_e}{9550},$$

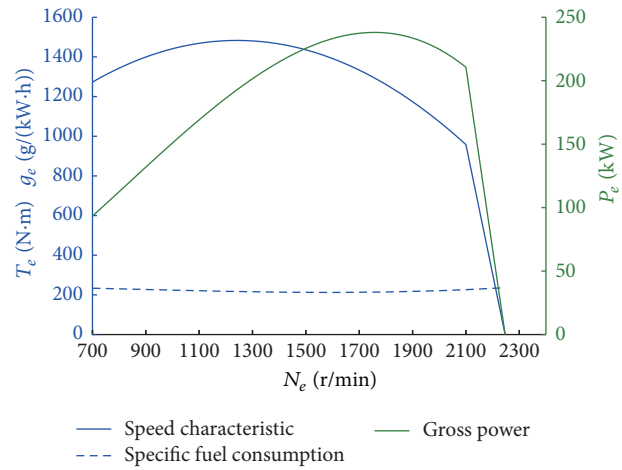


FIGURE 15: Engine throttle characteristics.

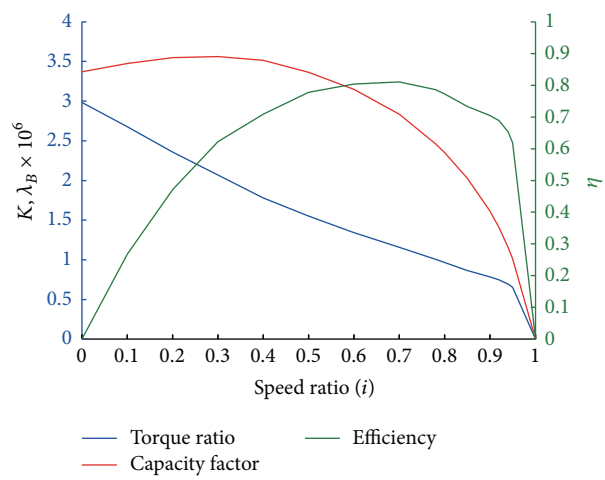


FIGURE 16: Original torque converter characteristics.

where $T_{e1}$ and $T_{e2}$ are engine torque, $P_e$ is engine power, $g_e$ is specific fuel consumption, and $a_i$, $b_i$, and $c_i$ are fitting coefficients. One has

$$\lambda_B = \sum_{j=0}^{n} a_j \cdot i^j,$$
$$K = \sum_{j=0}^{n} b_j \cdot i^j, \tag{12}$$
$$\eta = K \cdot i,$$

where $i$ is speed ratio, $\lambda_B$ is capacity factor, and $\eta$ is efficiency.

Vehicle force balance is calculated by

$$F_k = F_f + F_w + F_i + F_j, \tag{13}$$

where $F_k$ is traction force, $F_k = (T_T \cdot i_m \cdot \eta_m)/r_k$, $F_f$ is rolling resistance, $F_f = G \cdot \sin(\theta) \cdot f$, $F_w$ is wind resistance, $F_w = (C_D \cdot A \cdot u_a{}^2)/21120$, $F_i$ is slop resistance, $F_i = G \cdot \cos(\theta)$, and $F_j$ is acceleration resistance, $F_j = \delta \cdot m \cdot (du/dt)$.

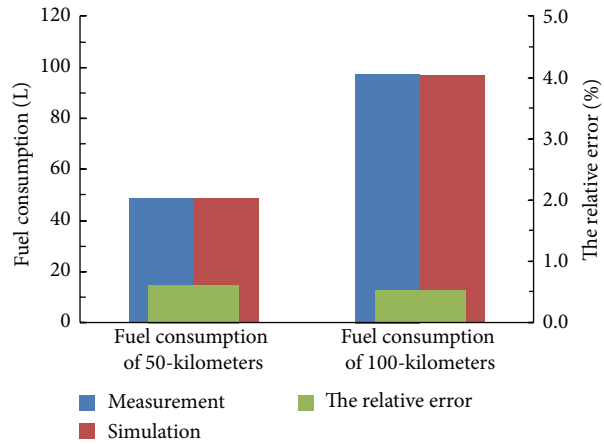


Figure 17: Fuel consumption comparison in the driving condition.

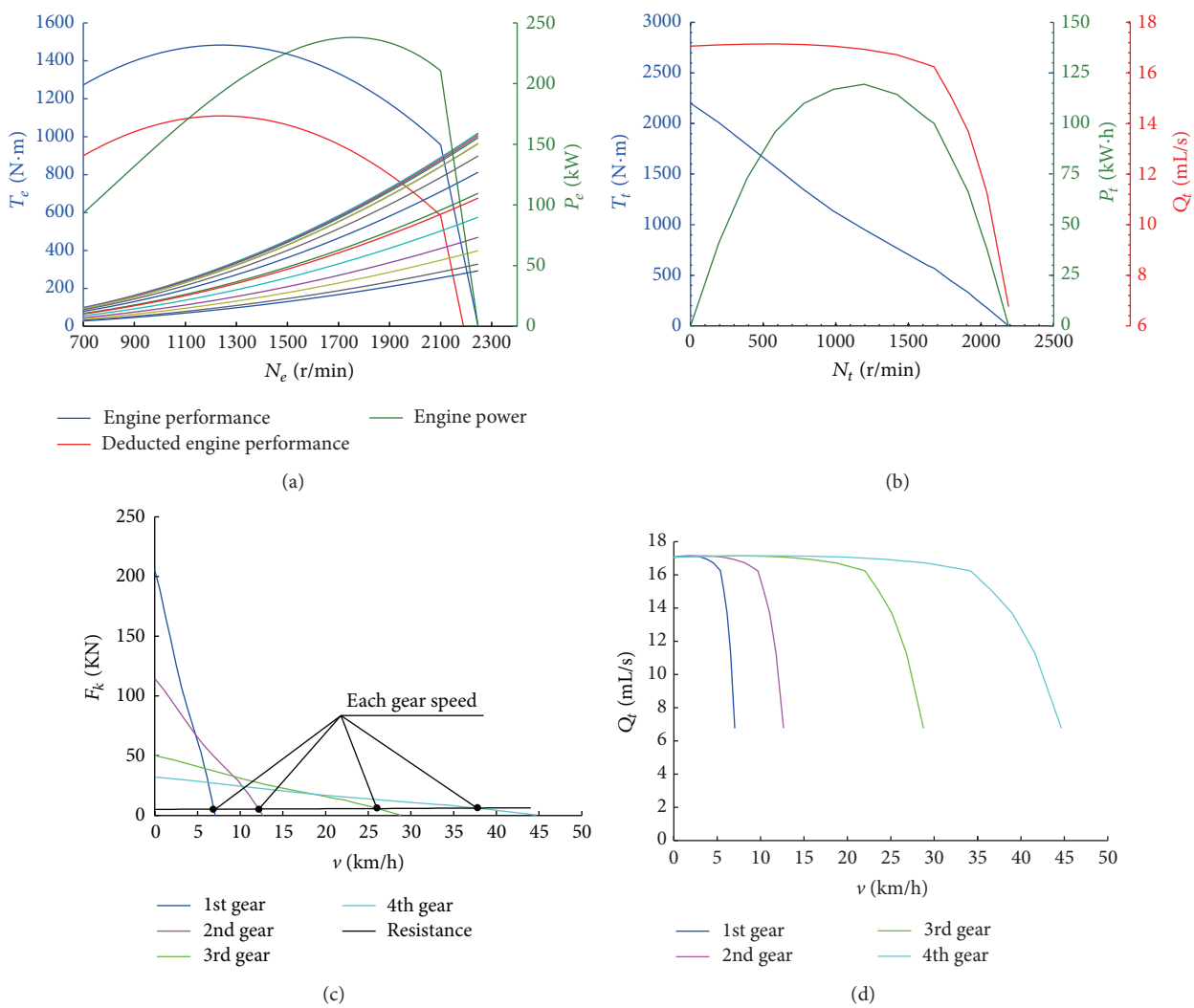


Figure 18: (a) Common input and (b) common output and (c) traction characteristic and (d) fuel consumption rate.

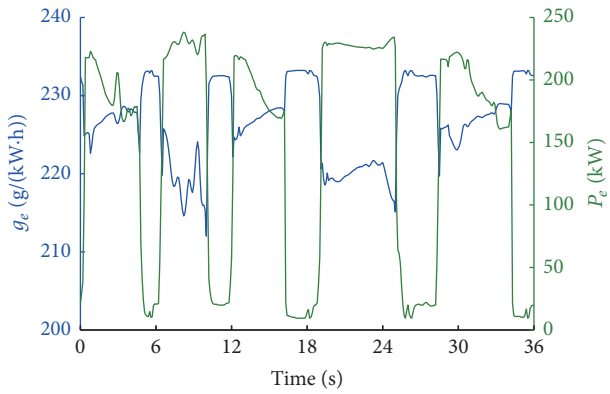


Figure 19: Engine dynamic output characteristics.

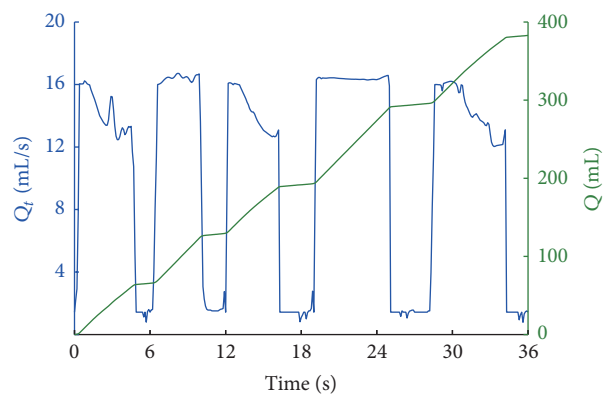


Figure 20: Dynamic fuel characteristics.

Fuel consumption ratio $Q_t$ can be calculated by

$$Q_t = \frac{P_e \cdot g_e}{367.1\rho g}, \tag{14}$$

where $\rho g$ is unit weight of fuel.

The fuel consumption mathematical model is the key to predict the fuel consumption of the V-type loading cycle. Comparing the calculated running fuel consumption based on (14) with testing data, as shown in Figure 17, we can see that the relative errors are 0.62% and 0.51%, respectively. The results show that the model is accurate for predicting the fuel consumption.

After extracting engine throttle and power deduction ratio at $t = 20$ s, the static matching performances are obtained (Figure 18).

After extracting the velocity and gear data at $t = 20$ s, the transient traction force $F_k$ and fuel consumption ratio $Q_t$ can be obtained by the interpolation method based on the traction characteristics and fuel consumption characteristics.

## 4. Simulation and Results

Figure 19 shows the engine output characteristics including dynamic engine gross power and specific fuel consumption. Figure 20 shows fuel consumption characteristics including fuel consumption ratio and total fuel consumption. Comparing Figure 19 with Figure 20, we can find that the tendency of vehicle fuel consumption characteristics is consistent with that of engine dynamic output characteristics. According to (14), fuel consumption ratio is proportional to the product of specific fuel consumption and engine output gross power. In the V-type loading cycle, the change of the specific fuel consumption is not large. Therefore, the engine output power is a crucial factor of fuel consumption ratio.

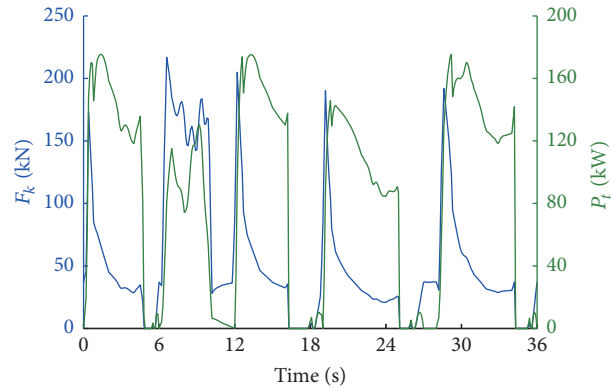


Figure 21: Dynamic traction characteristics.

Dynamic traction force reflects the vehicle dynamic performance in the V-type loading cycle to some degree. As shown in Figure 21, we can see that average output power of turbine shaft is higher in no-load or full-load running phases excluding V5 phase than that in V2 phase. The reason is that the lower velocity leads to the lower output power from turbine shaft in V2 phase, but the higher sticking force to insert material and the higher velocity in the running phase lead to the higher average output power in no-load and full-load running phases.

Fuel consumption comparison between test results and simulation results when loading different materials (freestone, sand, and stone) in the V-type loading cycle is shown in Figure 22. In general, the simulation curve fluctuates near the test curve which truly reflects the fuel consumption change in each phase of V-type loading cycle. The relative errors are calculated by (15) and the fuel consumption comparison is shown in Figure 23. Consider

$$e = \left| \frac{Q_0 - Q_1}{Q_0} \right| \times 100\%, \tag{15}$$

where $Q_0$ is the tested fuel consumption and $Q_1$ is the simulated fuel consumption.

As shown in Figure 23, the relative errors for various working conditions of loading freestone, sand, and stone are, respectively, 1.84%, 3.44%, and 2.03%, which are all lower than the required error in the engineering calculation, 5%. The result indicates that the loose degree of material is closely related to fuel consumption: the looser material means the lower fuel consumption.

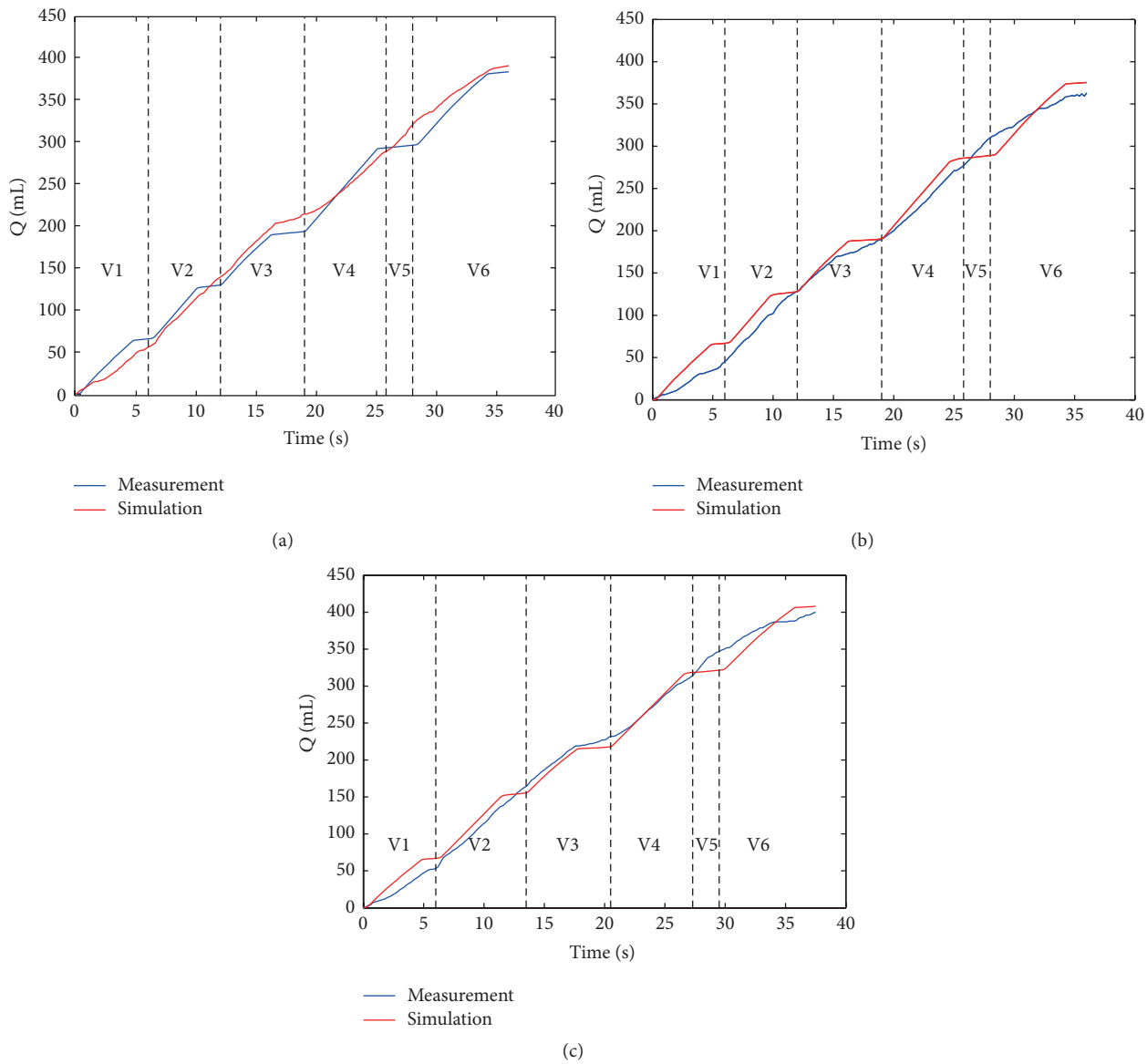


FIGURE 22: (a) Fuel consumption when loading freestone and (b) fuel consumption when loading sand and (c) fuel consumption when loading stone.

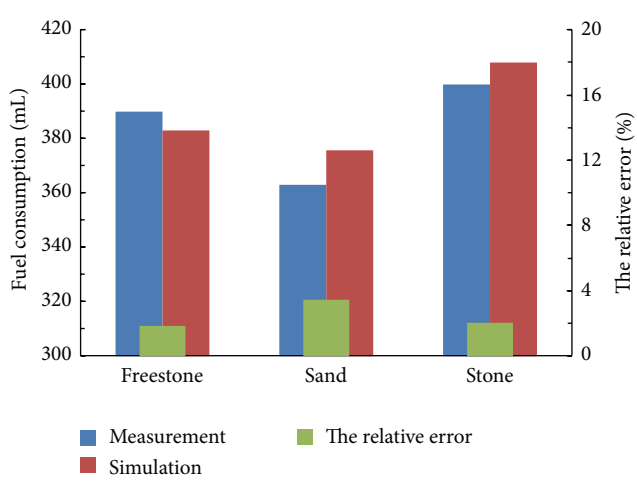


FIGURE 23: Loading fuel consumption comparison.

## 5. Conclusions

(1) The proposed method in this paper for predicting the fuel consumption of wheel loaders in the V-type loading cycle can accurately predict the fuel consumption in the V-type loading cycle. The relative errors for various working conditions of loading freestone, sand, and stone are, respectively, 1.84%, 3.44%, and 2.03%, which all meet engineering calculation requirements. The method can provide theoretical reference for design and optimization of wheel loaders.

(2) The model can not only predict the V-type loading fuel consumption but also provide the turbine shaft output power characteristics and vehicle dynamic output traction characteristics for judging whether the matching between engine and torque converter is reasonable.

(3) The dimensionless equations of engine power deduction based on the testing data provided the reference data for the design of wheel loaders.

## Conflict of Interests

The authors declare that there is no conflict of interests regarding the publication of this paper.

## Acknowledgment

This work was supported by the National High Technology Research and Development Program of China (863Program) (Grant no. 2014AA041502).

## References

[1] R. Filla, "An event-driven operator model for dynamic simulation of constructionmachinery," http://arxiv.org/abs/cs/0506033.

[2] C. Debeleac, "Vibratory diagnosis of the earthmoving machines for the additional necessary power level evaluation," in *Proceedings of the 9th WSEAS International Conference on Acoustics & Music: Theory & Applications (AMTA '08)*, pp. 24–26, Bucharest, Romania, June 2008.

[3] R. Filla, A. Ericsson, and J. O. Palmberg, "Dynamic simulation of constructionmachinery: towards an operator model," http://arxiv.org/abs/cs/0503087.

[4] R. Filla and J. O. Palmberg, "Using dynamic simulation in the development of construction machinery," http://arxiv.org/abs/cs/0305036.

[5] A. Hemami, "Motion trajectory study in the scooping operation of an LHD-loader," *IEEE Transactions on Industry Applications*, vol. 30, no. 5, pp. 1333–1338, 1994.

[6] W. Yossawee, T. Tsubouchi, S. Sarata, and S. Yuta, "Path generation for articulated steering type vehicle using symmetrical clothoid," in *Proceedings of the IEEE International Conference on Industrial Technology*, vol. 1, pp. 187–192, IEEE, 2002.

[7] L. Wu, *A study on automatic control of wheel loaders in rock/soil loading [Ph.D. thesis]*, University of Arizona, Tucson, Ariz, USA, 2003.

[8] S. Singh, *State of the Art in Automation of Earthmoving, 2002*, Carnegie Mellon University, 2002.

[9] J. A. Marshall, *Towards autonomous excavation of fragmented rock: experiments, modelling, identification and control [M.S. thesis]*, Queen's University, Kingston, Canada, 2001.

[10] M. Bohman, *On predicting fuel consumption and productivity of wheel loaders [M.S. thesis]*, Lulea University of Technology, Lulea, Sweden, 2006.

[11] H. Takahashi, "Simulation of the resistive forces acting on the bucket of wheel loader by use of DEM," in *Proceedings of the 5th International ISTVS Conference*, pp. 37–44, Seoul, Republic of Korea, 1998.

[12] R. Filla, *Operator and machine models for dynamic simulation of construction machinery [Ph.D. thesis]*, Linköping University, Linköping, Sweden, 2005.

[13] C. Debeleac, "Performances assessment from an earthmoving machine through power monitoring," *Annals of Dunarea de Jos University of Galati Fascicle XIV: Mechanical Engineering*, In press.

[14] K. S. Erer, "Adaptive usage of the Butterworth digital filter," *Journal of Biomechanics*, vol. 40, no. 13, pp. 2934–2943, 2007.

[15] R. G. T. Mello, L. F. Oliveira, and J. Nadal, "Digital Butterworth filter for subtracting noise from low magnitude surface electromyogram," *Computer Methods and Programs in Biomedicine*, vol. 87, no. 1, pp. 28–35, 2007.